J|A|C|S COMMUNICATIONS

Published on Web 09/01/2010

Size-Dependent Oxygen Activation Efficiency over $Pd_n/TiO_2(110)$ for the CO Oxidation Reaction

William E. Kaden, William A. Kunkel, Matt D. Kane, F. Sloan Roberts, and Scott L. Anderson*

Department of Chemistry, University of Utah, 315 South 1400 East, Room 2020, Salt Lake City, Utah 84112-0850

Received April 20, 2010; E-mail: anderson@chem.utah.edu

Abstract: The dissociative binding efficiency of oxygen over $Pd_n/TiO_2(110)$ ($n = 4, 7, 10, 20$) has been measured using temperature programmed reaction (TPR) mass spectrometry and X-ray photoemission spectroscopy (XPS) following exposure to O_2 with varying doses and dose temperatures. Experiments were carried out following two different O_2 exposures at 400 K (10 L and 50 L) and for 10 L of O_2 exposure at varying temperatures ($T_{surf} = 200$, 300, and 400 K). During TPR taken after sequential O_2 and CO (5 L at 180 K) exposures, unreacted CO is found to desorb in three features at $T_{desorb} \approx 150$, 200, and 430 K, while CO_2 is observed to desorb between 170 and 450 K. We show that Pd_{20} has exceptionally high efficiency for oxygen activation, compared to other cluster sizes. As a consequence, its activity becomes limited by competitive CO binding at low O_2 exposures, while other Pd_n sizes are still limited by inefficient O_2 activation. This difference in mechanism can ultimately be related back to differences in electronic properties, thus making this question one that is interesting from the theoretical perspective. We also demonstrate a correlation between one of the two CO binding sites and CO_2 production, suggesting that only CO in that site is reactive.

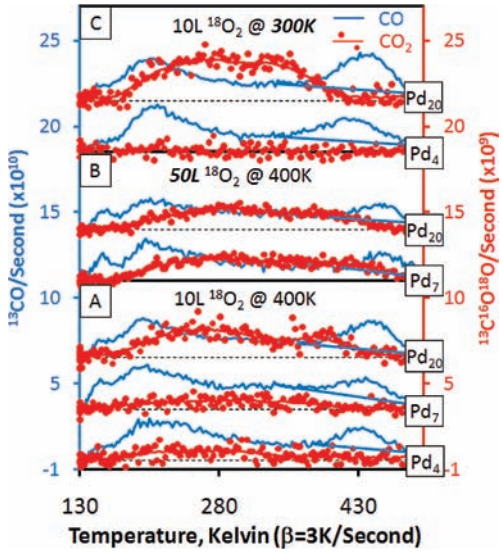

Figure 1. CO (left) and CO_2 (right) detected in TPR from Pd_n/TiO_2 ($n = 4, 7, 20$) after exposure to 10 L (A) and 50 L (B) of $^{18}O_2$ at 400 K, and 10 L of $^{18}O_2$ at 300 K (C). In all cases, the sample was subsequently dosed with 5 L of ^{13}CO at 180 K prior to recording the TPR. Details in text.

Over the past decade, much effort has been dedicated toward better understanding the role of particle size in determining the chemistry of the active sites in supported catalysts.[1−11] One of the most interesting size regimes is clusters of less than ∼30 atoms, where strong and nonmonotonic variations in activity with changing cluster size have been observed.[4−8,11] Recently, we reported a study showing, for the first time, a clear, one-to-one correlation between size-dependent CO oxidation activity of $Pd_n/TiO_2(110)$ ($n \leq 25$) and the Pd electronic structure as probed by X-ray photoemission (XPS).[12] Pd 3d binding energies (BEs) generally decrease with increasing size but fluctuate about this general trend. Clusters with higher-than-trend-BEs (Pd_7, Pd_4) show low activity, while clusters with high activity (Pd_{20}) have lower-than-trend BEs.[12] This correlation was observed for a particular set of reaction conditions, in which as-deposited clusters were first exposed to 10 L of O_2 at 400 K and then to 5 L of CO at 180 K, followed by measurement of CO_2 evolution as the samples were heated (3 K/s) in a temperature programmed reaction (TPR) run. The focus here is on the factors that control activity and, thus, determine the size dependence.

CO oxidation has been extensively studied on both Pd single crystals[13−16] and model Pd/oxide catalysts,[17−19] including size-selected Pd_n/MgO.[20,21] The Supporting Information briefly reviews relevant literature and includes additional experimental details. Here, we examine the effects of O_2 exposure and exposure temperature on activity for Pd_n/TiO_2 ($n = 4, 7, 10, 20$), prepared by soft landing (∼1 eV/atom) 1.53×10^{14} Pd/cm^2 (0.1 ML equivalent) in the form of preformed, mass-selected Pd_n^+, on vacuum-annealed $TiO_2(110)$[22−24] as detailed elsewhere.[25,26]

Figure 1 shows typical TPR data for select cluster sizes, O_2 exposures, and O_2 exposure temperatures. In each case, the samples were first exposed to $^{18}O_2$ and then to 5 L of ^{13}CO at 180 K and then cooled to 130 K and examined by TPR (3 K/s). Both residual CO (left axis) and CO_2 product (right axis) signals are shown. There are three CO desorption features. The small feature at ∼150 K is also observed without Pd and results from CO binding at oxygen vacancies or other defects on the TiO_2 support.[12,27] These "150 K" sites are populated by residual ^{13}CO as the sample is cooled from 180 to 130 K. Since the ^{13}CO exposure below 150 K is <0.05 L, it is evident that CO binding at defects must be facilitated by diffusion and capture of CO that initially lands on TiO_2 terrace sites. This effect is important when there is a small density of dispersed binding sites on a substrate where the adsorbate has a significant lifetime, as is the case for $CO/TiO_2(110)$.[21,22,28,29] If the O_2 pre-exposure is omitted, this ∼150 K desorption feature is enhanced, presumably because O_2 exposure blocks or heals ∼50% of the defects. The size of this feature is, however, independent of the presence of Pd_n, indicating TiO_2 defect blocking does not require O spillover from Pd to TiO_2.

The broad CO desorption features at ∼200 and ∼430 K are only observed if Pd_n clusters are present, indicating that CO binds in association with Pd in two different ways, with different desorption energies. $T_{desorption}$ of 430 K is similar to what has been reported for desorption of CO from 3-fold hollow sites on Pd(111);[15,30] thus

this CO is likely adsorbed directly on the Pd clusters. 200 K could correspond to CO in lower coordination bridge/atop sites but could also result from CO bound at the Pd−TiO_2 interface. A joint experimental/theoretical study of CO binding sites and energetics on Pd_n/TiO_2(110) is underway. Here we focus on the interplay between cluster size and changing oxidation conditions on CO adsorption and CO_2 production.

Figure 1 shows that Pd_{20} is the most active cluster for CO_2 production after 10 L O_2 exposure at 400 K (Figure 1A), with significantly lower activity for Pd_4 or Pd_7 (Pd_{10} is intermediate). Note that the CO_2 yield is <10% of the total CO signal, indicating that most CO adsorbing at 180 K desorbs without reacting under these conditions. No additional CO desorption is seen for heating up to $T_{Surface} = 800$ K, and XPS and ISS show no signs of residual carbon on the surface after TPR.

The onset temperature for CO_2 evolution (~170 K) is well above the CO_2 desorption temperature (~130 K) observed when CO_2 is adsorbed on Pd_n/TiO_2 at low temperatures, and there is no evidence of stably adsorbed CO_2 species formed in higher temperature CO_2 exposures. Therefore the temperature dependence of CO_2 evolution reflects the kinetics for production of CO_2 from CO and O adsorbed on these samples, consistent with observations made for single crystal surfaces.[13−15] In that case the broad temperature range over which CO_2 is observed suggests that there is a broad range of activation energies for reaction of CO_{ads} and O_{ads}, presumably reflecting a range of CO and/or O adsorption sites occupied as the surface concentrations of the reactants change throughout the reaction. The fact that the ~170 K onset temperature is cluster-size-independent simply reflects the fact that CO exposure was made at 180 K, such that any CO in sites with low activation energies is reacted away. We do measure CO_2 evolution during the CO exposure, and in all cases, this <170 K CO_2 production accounts for <10% of the total CO_2 production in TPR. (The 180 K CO exposure temperature was chosen to avoid CO adsorption on TiO_2 terrace sites.)

We detect no O_2 desorption during the CO dose or subsequent TPR; however, we do have some insight into the nature of the adsorbed oxygen generated under the conditions used here (10−50 L exposures at 200−400 K): (1) ISS indicates that oxygen adsorbs on Pd sites (attenuating Pd signal ~50%) and that this Pd-bound oxygen is not removed by heating up to 500 K, unless CO is also present, in which case it is reacted away. (2) Pd XPS shifts to higher BE upon O_2 exposure (vide infra). (3) There is no significant change in Ti XPS, but ISS shows ^{18}O incorporation into the TiO_2 surface layer after TPR. The ^{18}O amount is independent of the presence of Pd. (4) After TPR, subsequent CO exposure and TPR produce no CO_2 unless the sample is also re-exposed to O_2 before TPR. If subsequent TPR includes O_2 re-exposure, CO_2 production is observed. These data show that oxygen adsorbs on Pd, oxidizing it, and that 5 L CO exposure with heating to 500 K removes all the Pd-bound oxygen. Furthermore, spillover of O to the TiO_2 support is negligible under our conditions, in contrast to previous experiments where O spillover was observed, albeit with 500 L of O_2 exposure at >550 K.[31]

Previously, we noted that the amount of CO_2 produced from Pd_n/TiO_2 in TPR (10 L of O_2 at 400 K, 5 L of CO at 180 K) appeared to be correlated with the intensity of unreacted CO desorbing in the higher temperature ("430 K") feature, whereas the lower temperature desorption features appear uncorrelated with CO_2 production.[12] To examine this correlation more quantitatively for different oxidation conditions, it is useful to subtract out the tail extending into this temperature range from the lower temperature desorption features, which we have done crudely

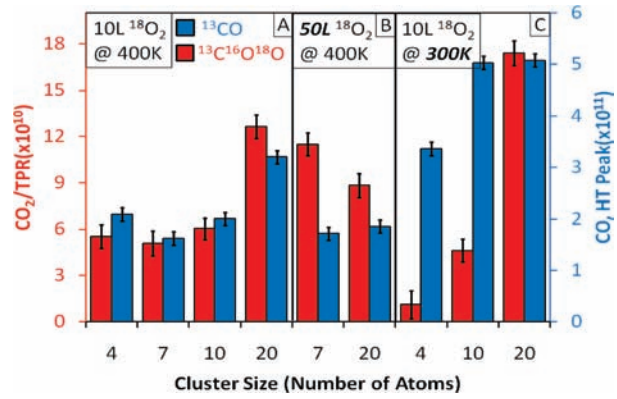

Figure 2. Comparisons of ~430 K CO desorbing (background subtracted) with total CO_2 detected during TPR for samples exposed to 10 L of O_2 at 400 K (A), 50 L of O_2 at 400 K (B), and 10 L of O_2 at 300 K (C). All samples were subsequently exposed to 5 L of CO at 180 K prior to TPR.

by simply extrapolating a baseline (sloping blue lines in Figure 1). Figure 2 compares the absolute CO_2 yield (left scale) with the baseline-subtracted 430 K CO desorption (right scale). Note that, for 10 L 400 K O_2 exposure (Figure 2A), the correlation is reasonably good, such that the ratio of CO_2 to "430 K CO" is ~1 to 3; i.e., ~25 ± 5% of the 430 K CO is reacted to CO_2, approximately independent of cluster size.

The cluster size dependence of the CO_2 yield, as well as the correlation with 430 K CO, is strongly dependent on O_2 exposure and exposure temperature, as shown in Figure 1B and 1C and Figure 2B and 2C. Data are given for the cluster size that is most active for 10 L 400 K O_2 exposure (Pd_{20}) and for either Pd_7 or Pd_4, which are clusters with similar, much lower activity under those conditions. In Figures 1B and 2B, the O_2 exposure prior to TPR was increased to 50 L at 400 K. If CO_2 production is limited by oxygen activation kinetics, then we would expect increased CO_2 production at 50 L O_2 exposure. This is clearly the case for Pd_7; the integrated CO_2 yield (Figure 2) increases by a factor of ~2 compared to the 10 L experiment. In contrast, for Pd_{20}, the CO_2 yield *decreases* ~30% for 50 L O_2 exposure, such that Pd_7 is now more active than Pd_{20}. Note also that the total amount of CO desorbing from both samples is significantly lower for 50 L O_2 exposure, compared to the 10 L O_2 experiment. Figure 2B also shows that the intensity of the residual 430 K CO desorption is substantially lower for Pd_{20} but not for Pd_7. The ratio of CO_2 to unreacted 430 K CO is substantially higher for 50 L O_2 exposure, as might be expected; however, for Pd_{20}, less CO adsorbs, resulting in lower CO_2 yield. This behavior suggests that, for Pd_{20}, the higher O_2 exposure pushed the system into the kinetic regime where CO_2 yield is inhibited by partial blocking of CO binding sites by O_{ads}.

The increase in CO_2 yield for Pd_7 after the higher O_2 exposure suggests that O_2 adsorption/activation is significantly less efficient than the case for Pd_{20}, and perhaps the origin of the previously observed size-dependent CO oxidation activity can be attributed mostly to variations in efficiency of the O_2 activation, under the rather mild 400 K 10 L O_2 exposures. The additional O_{ads} generated with larger exposure leads to more efficient oxidation of CO_{ads}, but the O_{ads} is still not dense enough to significantly inhibit CO adsorption into the 430 K feature.

To verify that additional O_2 exposure results in additional O_{ads} on Pd, we measured XPS following oxidation of Pd_7 and Pd_{20} with 10 and 50 L doses at 400 K. Figure 3 shows the shifts in the Pd 3d BE relative to the BE observed for freshly prepared samples. For 10 L of O_2, the oxidative shift is larger for Pd_{20} than for Pd_7,

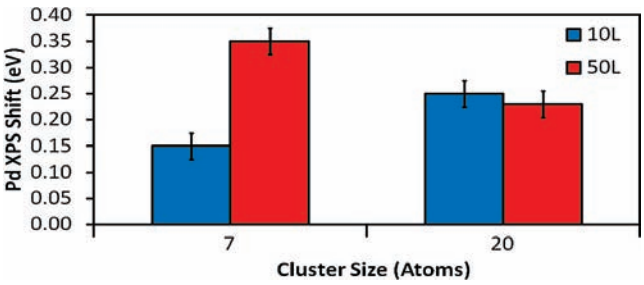

Figure 3. Shifts in the Pd 3d XPS peak position for Pd_7 and Pd_{20} samples after exposure to 10 and 50 L of O_2 at 400 K. Shifts are relative to the binding energies for as-deposited samples.

consistent with our conclusion that Pd_{20} is more efficient at adsorbing/activating oxygen. For 50 L exposure, Pd_7 shows a substantially increased shift, consistent with additional Pd oxidation. For Pd_{20} there is no additional shift, suggesting that even, for 10 L of O_2, the cluster is already as oxidized as it can get at 400 K. Apparently at higher O_2 exposures there are some additional changes that partially block CO adsorption but do not result in any further shift in the Pd electronic properties. For example, molecular O_2 might bind to the oxidized Pd_{20}, or there might be a change in cluster structure that leaves fewer CO binding sites. XPS shifts depend not only on oxidation state but also on screening/relaxation in the photoemission final state, which may vary with cluster size, oxidation state, and interaction with the support. Therefore, it is not possible to assign the shifts to a particular Pd_nO_m stoichiometry.[32,33] Nonetheless, the relatively small shifts following O_2 exposure suggest that we are forming something like Pd with adsorbed O, rather than a true oxide, such as what forms in higher temperature O_2 exposures[19,34] (bulk PdO and PdO_2 are shifted ~1 and ~3 eV relative to bulk Pd).[35]

If dissociative oxygen adsorption is an activated process, its efficiency should be highly dependent on the O_2 exposure temperature. Figures 1C and 2C show the effects of lowering the temperature to 300 K for a 10 L O_2 exposure. For all cluster sizes investigated, the intensity of unreacted CO desorbing during TPR increases substantially, and the same is true for the 430 K component of the CO signal (Figure 2C). This increase is consistent with less CO site blocking for 300 K oxidation. For Pd_{20}, which was already the most active cluster size for 400 K oxidation, the CO_2 yield increases substantially for 300 K oxidation, indicating that, even at 400 K, this cluster is overoxidized, with significant CO site blocking. In contrast, for Pd_4 and Pd_{10} (shown only in Figure 2C) lower oxidation temperature substantially reduces CO_2 yield, even though the amount of CO adsorbed is substantially greater than that for 400 K oxidation. Experiments were also carried out with 10 L O_2 exposure at 200 K, and no CO_2 production was detected, even for Pd_{20}, demonstrating that formation of the reactive oxygen (O_{ads}) is an activated process for all our clusters. Activated O_2 adsorption has been observed on both supported Pd and some single crystal surfaces (see Supporting Information). The novel observation here is that the activation energy varies strongly and nonmonotonically with cluster size, with efficiency decreasing again as size increases above Pd_{20}.

In the context of interpreting the previously reported size dependence, it seems clear that, for most of the clusters, activated oxygen adsorption was the limiting factor that largely determined the size dependent activity. Additionally, the CO_2 yield appears to be correlated with the amount of CO in the higher temperature (430 K) binding site, and conversion of this CO to CO_2 occurs with reasonable efficiency for all cluster sizes, provided oxygen is present to react with. The exception is Pd_{20}, where 10 L at 400 K already takes the system into the regime where CO adsorption starts to be the limiting factor. By varying O_2 exposure and exposure temperature, the Pd_n/TiO_2 system can be driven from O-limited to CO-limited kinetic regimes, and the transition is strongly dependent on cluster size. For this reason, the size dependence of the activity is also highly dependent on O_2 exposure conditions. For example, the Pd_{20}/Pd_4 activity ratio is ~2.3 for 10 L of O_2 and 400 K but increases to ~16 for 10 L of O_2 at 300 K.

That the smaller clusters appear to be generally less efficient at oxygen activation appears consistent with the idea that O adatoms tend to bind in highly coordinated sites on single crystals,[15] as the small clusters are expected to have fewer high coordination sites. Note, however, that the size dependence is nonmonotonic (e.g., Pd_{16} and Pd_{25} are both substantially less active than Pd_{20} for 10 L of O_2 at 400 K).[12] In addition, small Pd_n bind to TiO_2 in the form of mostly single layer islands where the number of Pd atoms exposed in the surface layer (as seen by ISS) varies slowly (and monotonically) with size. Another factor expected to influence oxygen activation is electronic structure, and as noted, this system shows fluctuations in Pd 3d BE that correlate strongly with activity. Tentatively, therefore, we attribute the variation in O_2 activation efficiency to variations in electron structure with size.

Acknowledgment. Funding for this work has been provided by AFOSR Grant FA9550-08-1-0400.

Supporting Information Available: Summary of background literature. Experimental Details. Complete citations for all references. This material is available free of charge via the Internet at http://pubs.acs.org.

References

(1) Valden, M.; Lai, X.; Goodman, D. W. *Science* **1998**, *281*, 1647–1650.
(2) Matthey, D.; Wang, J. G.; Wendt, J. G.; Matthiesen, J.; Schaub, R.; Laegsgaard, E.; Hammer, B.; Besenbacher, F. *Science* **2007**, *315*, 1692–1696.
(3) Lemire, C.; Meyer, R.; et al. *Surf. Sci.* **2004**, *552*, 27–34.
(4) Lee, S.; Fan, C.; Wu, T.; et al. *J. Am. Chem. Soc.* **2004**, *126*, 5682–5683.
(5) Sanchez, A.; Abbet, S.; et al. *J. Phys. Chem. A* **1999**, *103*, 9573–9578.
(6) Landman, U.; Yoon, B.; et al. *Top. Catal.* **2007**, *44*, 145–158.
(7) Buratto, S. K.; Bowers, M. T.; et al. *Chem. Phys. Solid Surf.* **2007**, *12*, 151–199.
(8) Vajda, S.; Pellin, M. J.; et al. *Nat. Mater.* **2009**, *8*, 213–216.
(9) Herzing, A. A.; Kiely, C. J.; et al. *Science* **2008**, *321*, 1331–5.
(10) Fu, Q.; Saltsburg, H.; et al. *Science* **2003**, *301*, 935–938.
(11) Wang, J. G.; Hammer, B. *Phys. Rev. Lett.* **2006**, *97*, 136107–136111.
(12) Kaden, W. E.; Wu, T.; et al. *Science* **2009**, *326*, 826–830.
(13) Engel, T.; Ertl, G. *Chem. Phys. Lett.* **1978**, *54*, 95–98.
(14) Engel, T.; Ertl, G. *J. Chem. Phys.* **1978**, *69*, 1267–1281.
(15) Conrad, H.; Ertl, G.; Kueppers, J. *Surf. Sci.* **1978**, *76*, 323–342.
(16) Hanley, L.; Guo, X.; et al. *J. Chem. Phys.* **1989**, *91*, 7220–7227.
(17) Shaikhutdinov, S.; Heemeier, M. *Surf. Sci.* **2002**, *501*, 270–281.
(18) Brandt, B.; Schalow, T.; et al. *J. Phys. Chem. C* **2007**, *111*, 938–949.
(19) Schalow, T.; Brandt, B.; et al. *Phys. Chem. Chem. Phys.* **2007**, *9*, 1347–1361.
(20) Harding, C. J.; Kunz, S.; et al. *Phys. Chem. Chem. Phys.* **2008**, *10*, 5875–5881.
(21) Kunz, S.; et al. *J. Phys. Chem. C* **2010**, *114*, 1651–1654.
(22) Lee, S.; Fan, C.; et al. *J. Chem. Phys.* **2005**, *123*, 124710–124723.
(23) Epling, W. S.; Peden, C. H. F.; et al. *Surf. Sci.* **1998**, *412/413*, 333–343.
(24) Diebold, U.; Li, M.; et al. *Surf. Rev. Lett.* **2000**, *7*, 613–617.
(25) Aizawa, M.; Lee, S.; et al. *J. Chem. Phys.* **2002**, *117*, 5001–5011.
(26) Aizawa, M.; Lee, S.; et al. *Surf. Sci.* **2003**, *542*, 253–275.
(27) Linsebigler, A.; Lu, G.; et al. *J. Chem. Phys.* **1995**, *103*, 9438–43.
(28) Kaden, W. E.; et al. *J. Chem. Phys.* **2009**, *131*, 114701–114715.
(29) Bowker, M.; Stone, P.; et al. *Surf. Sci.* **2002**, *497*, 155–165.
(30) Kok, G. A.; Noordermeer, A.; et al. *Surf. Sci.* **1983**, *135*, 65–80.
(31) Bowker, M.; Fourre, E. *Appl. Surf. Sci.* **2008**, *254*, 4225–4229.
(32) Takasu, Y.; Unwin, R.; et al. *Surf. Sci.* **1978**, *77*, 219–232.
(33) Mason, M. G. *Phys. Rev. B* **1983**, *27*, 748–762.
(34) McClure, S. M.; Goodman, D. W. *Chem. Phys. Lett.* **2009**, *469*, 1–13.
(35) Moulder, J. F.; et al., eds. *Handbook of X-ray Photoelectron Spectroscopy*; Physical Electronics: Eden Prarie, MN, 1995.

JA103347V